Electrical and thermal properties of highly quenched amorphous V_2O_5 thin films

J. P. AUDIERE, A. MADI
Université Paris Sud, Laboratoire de Physicochimie Minérale, Bâtiment 420, 91405 Orsay, France

J. C. GRENET
Laboratoire de Magnetisme, 92190 Meudon, France

Amorphous thin films of V_2O_5 have been prepared by vapour deposition in high vacuum ($\sim 10^{-6}$ torr). In order to study the role of quenching, various temperatures, ranging from -196 to $260°$ C, have been selected for the substrate. Differential thermal analysis, X-ray diffraction and conductivity measurements clearly divide the material into two sets, depending on the efficiency of the quenching. Whereas the least-quenched samples resemble those previously obtained by splat-cooling, the better quenched are only barely stable and, as a consequence, exhibit unique features, such as the occurrence of a glassy transition and the highest crystallization temperature ever found for V_2O_5.

1. Introduction

Many papers have been devoted to amorphous vanadium pentoxide in view of its interesting semiconducting properties. However, most studies till now have been performed on bulk amorphous materials obtained either by splat-cooling [1], by dehydration of a gel [2–4] or on thin films obtained by chemical vapour deposition [5, 6]. Apart from the works [7–10] on crystalline and amorphous vanadium pentoxide obtained by sputtering or vapour deposition, no extensive research has been published on amorphous material prepared by evaporation, nor has the effect of the efficiency of quenching been studied. The object of the present work was to prepare thin films with a small V^{4+}/V^{5+} ratio and to study the effect of heat tréatment of the material on the conductivity, as a function of the mode of preparation.

2. Experimental techniques

The amorphous thin layers were made by vacuum evaporation ($P \sim 10^{-6}$ torr) of powdered vanadium pentoxide (Johnson-Matthey, Specpure) placed in an electrically heated crucible. The corrosive nature of molten vanadium pentoxide requires the use of a platinum crucible and platinum/rhodium–platinum thermocouples. The temperature of the molten oxide, which is the main parameter responsible for the composition of the vapour [11, 12], was carefully controlled [13]. Thin layers, as close to stoichiometry as possible ($V^{4+}/V^{5+} \sim 0.01$–0.02), were chosen for study. Since the dissociation of the vanadium pentoxide occurs as: $V_2O_5 \rightleftharpoons V_2O_{5-x} + (x/2)O_2$ [2], it was necessary to conduct a comparative study of thin layers with the same V^{4+}/V^{5+} ratio and free from oxides such as V_3O_7, V_4O_9 or V_6O_{13} (which limits the V^{4+}/V^{5+} ratio to a maximum of about 0.02 [2, 14–16].) In a first series of experiments, the temperature of the crucible was fixed at about $845 \pm 5°$ C, a reasonable compromise between a low dissociation and a suitable rate of evaporation. The films obtained were pale yellow.

In a second series of experiments, the V^{4+}/V^{5+} ratio was increased by evaporating at $900 \pm 10°$ C, in order to study the influence of evaporation temperature. The films thus obtained were dark yellow. The very small mass of amorphous evaporated films did not allow us to measure the V^{4+}/V^{5+} ratio. However, the colour suggested the presence of only a very small amount of V^{4+} (certainly $< 2\%$). The glass platelets (50 mm ×

0022–2461/82/102973–06$03.22/0

50 mm × 0.5 mm) used as substrates were first degreased, chemically scoured and refluxed in 2-propanol. They were then degassed at 250° C for 3 h under high vacuum, and immediately used for the evaporation. The substrates were mechanically held on a substrate holder, and the temperature of both was regulated in the − 196 to 450° C temperature range [11]. The temperature difference between the V_2O_5 glass interface and the substrate holder was less than 0.5° C [13]. In some cases, it was necessary to intercalate between the substrate and the thin layer of oxide a thin film of gold (about 15 nm) to allow the subsequent removal of the oxide layer, which was otherwise held tenaciously. The evaporation apparatus was thus provided with two sources, one for the pentoxide and the other for gold flash evaporation. After preparation, the layers were stored under vacuum to protect them from moisture [4, 17]. In an attempt to gauge the possible influence of moisture, a film (no. 7) obtained by vapour deposition onto a substrate maintained at liquid nitrogen temperature was voluntarily exposed to ambient atmosphere while kept at 0° C: it underwent immediate hydration. Differential thermal analysis (DTA) of about 0.5 mg samples scraped from the substrate turned out to be possible using microcrucibles in the DTA [18]. The thermograms (Fig. 1) were obtained with a 7.5° C min^{-1} heating rate, under inert atmosphere. When required, a special device allowed *in situ* forced cooling of the sample at a rate of about 10–20° C min^{-1} [18, 19].

The evolution of the crystallinity of the samples was followed by optical microscopy and X-ray diffractometry. Dark-field optical microscopy permitted the detection of crystallites larger than 0.3 μm, even if they were dispersed in the amorphous phase. This technique also allowed the localization of crystallites with reference to the air–V_2O_5 and V_2O_5 glass interfaces [13, 20].

Thickness measurements were performed using a Mirot interferometer and an interference filter (546 nm) equipped with a camera. Under these conditions, the film thickness could be estimated to within ± 5% for the very thick layers (i.e. more than 270 nm thick), and to within ± 10% for the very thin layers. Direct examination of the thin films was performed by X-ray diffractometry (Siemens, Cu$K\alpha_1$). The samples which had to be scraped off for DTA were examined with a Seeman–Bohlin camera.

In order to measure the conductivity of the samples, two parallel gold electrodes were deposited onto the pentoxide films. The distance between the electrodes (typically 300 μm) was measured with an optical microscope and chosen to be a suitable compromise between too large resistance and too high electric field. Fig. 2 gives a diagram of the apparatus used for electrical measurements. The high resistance Rx of the sample limited the value of the current delivered by a stabilized d.c.

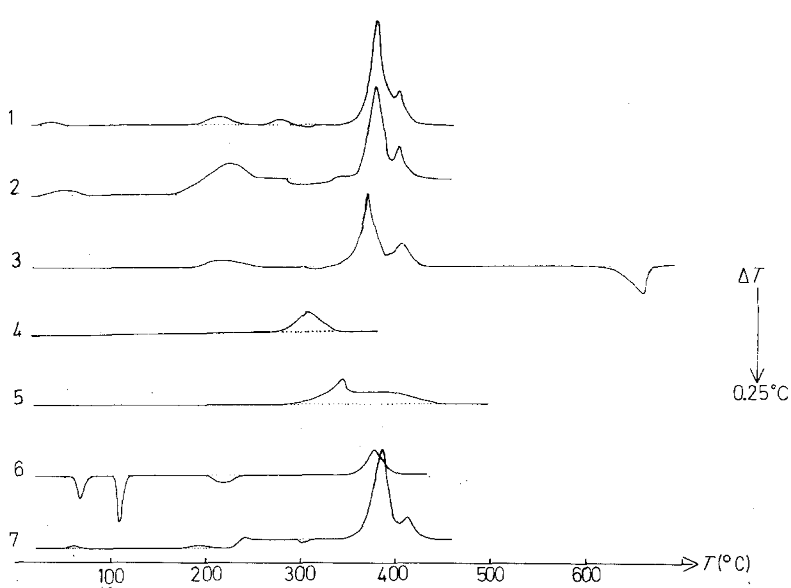

Figure 1 DTA thermograms of samples 1 to 7. Sample 1, mass = 0.63 mg; 2, 0.7 mg; 3, 0.6 mg; 4, 0.3 mg; 5, 0.7 mg; 6, 0.73 mg; 7, 0.48 mg.

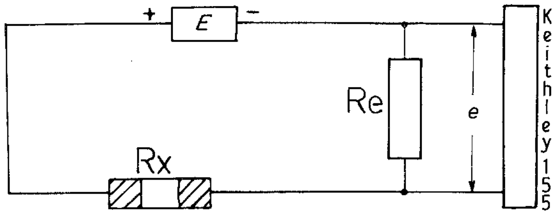

Figure 2 Diagram of apparatus used for electrical measurements.

generator E. The potential difference across a reference resistance Re (Re ≪ Rx), was then measured using the Keithley 155 microvoltmeter. For all measurements, the potential E was fixed between 9 and 10 V. It was systematically verified that this value was in good agreement with ohmic behaviour. The heating rate during the conductivity measurements was about 3° C min^{-1}.

3. Results and discussion

Preparation parameters are reported in Table I.

3.1. DTA and X-ray diffractrometry results

The thermograms of the seven selected preparations are reported in Fig. 1. Thermograms 1, 2, 3 and 7 are very similar. The main exothermic peak begining at about 340° C was attributed to crystallization.

In all cases, anneals followed by quenching from various temperatures were systematically performed. The samples were then examined by optical microscopy and X-ray diffractometry. After quenching from 290° C, the material was still amorphous. After quenching from 335° C, the X-ray pattern exhibited a weak, but sharp line which proved to be the (001) line of the orthorhombic vanadium pentoxide ($a = 1.151$ nm, $b = 0.3559$ nm and $c = 0.4371$ nm [21]). By subsequent studies after quenching from 380° C, the X-ray patterns showed a series of sharp $(h0l)$ lines in addition to very diffuse (hkl) lines ($k \neq 0$). After quenching from 420° C, crystallization was found to be complete; all the lines of the X-ray pattern were sharp and were indexed as due to orthorhombic V_2O_5. The suggested explanation takes into account both the lamellar and the chain nature of V_2O_5 (Fig. 3). The appearance at first of the (001) reflection suggests a regular stacking of imperfect *ab* planes; the subsequent appearance (380° C) of the $(h0l)$ lines is related to organization of the "in plane" V–O–V chains, the VO_5 square pyramids still having some irregularity. Finally, complete crystallization is achieved at 420° C.

The hydrated layer (no. 6) showed a particular mode of behaviour, similar to that observed for the gel [4, 17]. It crystallized at once at about 350° C and exhibits three successive dehydrations.

The shape of the peaks of crystallization for Samples 4 and 5 suggests a mechanism of crystallization with simultaneous nucleation and growth, in contrast to the three-step process observed with Samples 1, 2, 3 and 7. As the DTA runs were performed under inert atmosphere, and since Samples 1, 2, 3 and 7 were amorphous at 290° C, it clearly appeared that the weak exothermic peaks observed in the 40–290° C temperature range were due to relaxations between different amorphous states (Fig. 4). We note that the relaxations observed on Thermogram 7 were a little enhanced with respect to those observed on Thermogram 2 in relation to the higher V^{4+}/V^{5+} ratio of 7. Annealing at fixed temperature t_x suppressed all the relaxation processes observed at $t < t_x$. Thermograms 3 and 5 illustrate this type of behaviour, commonly encountered in the field of amorphous materials [18].

The originality of our evaporated films as compared to samples of V_2O_5 previously prepared

TABLE I

Thin film number	Evaporation temperature (° C)	Substrate temperature (° C)	Remark
1	840	−196	Stored under vacuum
2	840	20	Stored under vacuum
3	840	127	Stored under vacuum
4	840	185	Stored under vacuum
5*	840	260	Stored under vacuum
6	840	−196	Hydrated for a few seconds with air moisture
7	900	20	Stored under vacuum

* It was impossible to scrape off this layer.

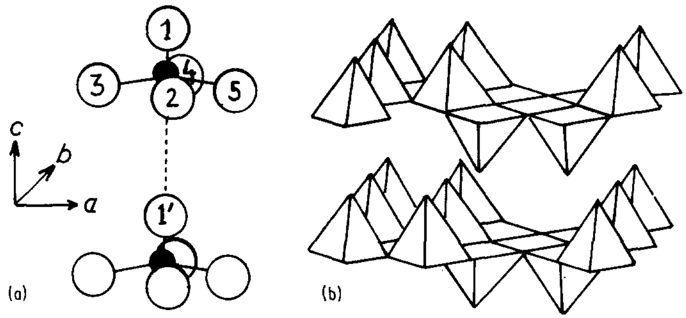

Figure 3 Structure of V_2O_5. (a) Square pyramids VO_5: $V{-}O_1 = 0.158$ nm, $V{-}O_2 = V{-}O_4 = 0.188$ nm, $V{-}O_3 = 0.178$ nm, $V{-}O_5 = 0.202$ nm, $V{-}O_{1'} = 0.278$ nm. (b) Chains of square pyramids in the *ab* plane.

appears as a weak endothermic signal at about 300° C on Thermograms 1, 2, 3 and 7. This signal is attributed to the glass transition occurring at the temperature T_g, which has not been reported so far. Basically, the presence of a glass transition in our samples is connected with the very rapid cooling rate during preparation of our samples which prevented the formation of any micro-crystallites, and this results in a high crystallization temperature. Amorphous V_2O_5 obtained by splat-cooling crystallizes at about 240° C, far below the glass transition T_g [17]. The small exothermic effect observed just before T_g (Fig. 1, Thermograms 1, 2, 3 and 7) is presumably due to some relaxation towards a more stable glassy state in the vicinity of T_g before the glass returns to the equilibrium in liquid state. In agreement with a well-known rule, we note that the temperature T_g (~ 585 K) is about two-thirds of melting (~ 885 K). A last striking difference in our samples is the melting temperature, which is much lower than usual (i.e. in bulk material) (690° C) [22]. This is connected with surface effects which of course are of crucial importance on a 250 nm thick sample. This is borne out by similar cases previously reported [13].

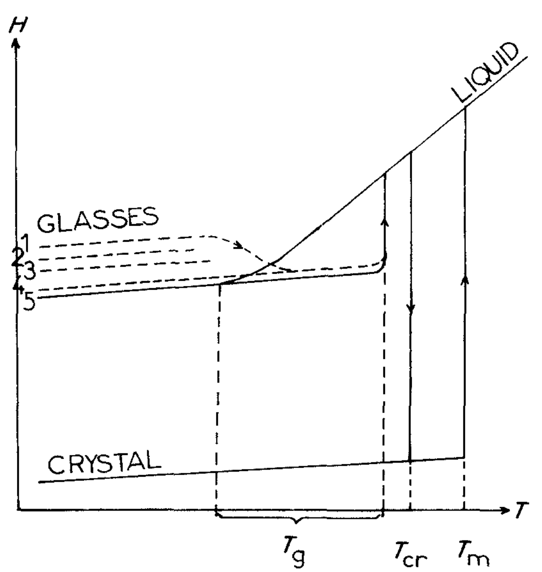

Figure 4 Enthalpy H versus absolute temperature T diagram. T_g = glass transition temperature; T_{cr} = crystallization temperature; T_m = melting temperature.

3.2. Conductivity results

The values of log σT versus the reciprocal absolute temperature for Layers 1 to 5 are reported in Fig. 5. A striking feature is that the conductivity strongly depends on the degree of quenching: the weaker the quenching, the higher the conductivity. The curves may be divided into two sets: in the first set (Curves 5 and 4), the slope of the logσT

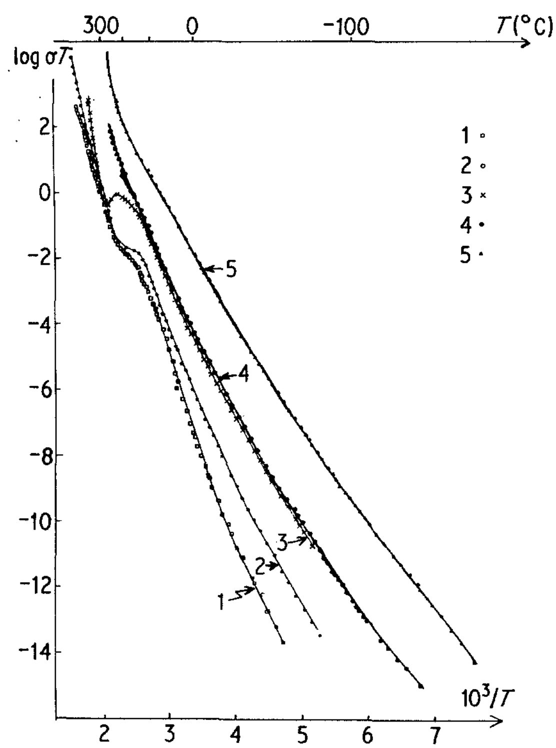

Figure 5 log σT versus $10^3/T$ for Layers 1 to 5 (σ in Ω^{-1} cm^{-1}; T in degree Kelvin).

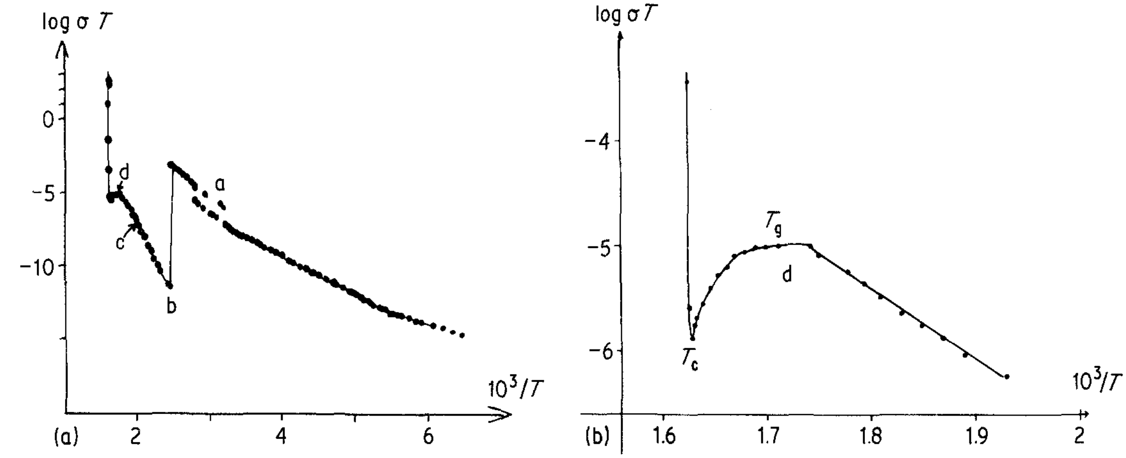

Figure 6 (a) log σT versus $10^3/T$ for Sample 7. (b) Enlargement of (a).

versus $10^3/T$ curves suddenly increases above 180° C ($10^3/T < 2.25\ K^{-1}$) because of the onset of crystallization. In the second set (Curves 3, 2, 1), the initial slope is steeper and presents several discontinuities of slope in the temperature range $|10^3/T \sim 2.7$ to $2.2\ K^{-1}|$. In addition, a much lower conductivity is found. It is worth noting that Curve 5 (Fig. 5) is extremely similar to the one obtained for a xerogel [23]. For the sake of clarity, the conductivity of Sample 7 (prepared with a higher vapour temperature) is shown separately on Fig. 6a. Several discontinuities are observed at temperatures corresponding to the glass relaxations observed in DTA. In addition, Fig. 6b shows an enlargement of Fig. 6a in the range ($1.6 \leqslant 10^3/T \leqslant 1.9\ K^{-1}$). The conductivity anomaly is clearly related to the onset of the glass transition followed by the occurrence of crystallization at higher temperature. Finally, it is interesting to show in detail the behaviour of the conductivity in the crystallization range. Figs. 7a and b show a plot of log σT and σ versus $10^3/T$ in the case of Sample 2.

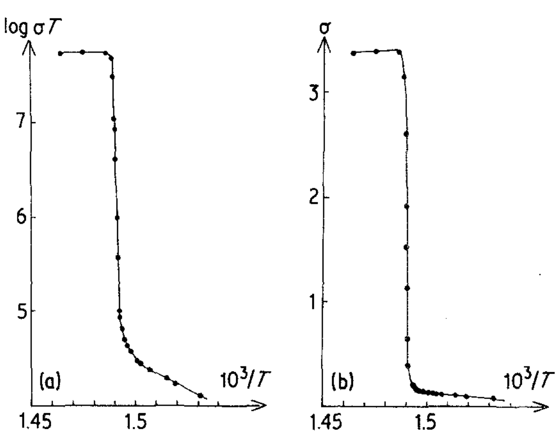

Figure 7 (a) log σT versus $10^3/T$ for Sample 7 in the crystallization vicinity. (b) σ versus $10^3/T$ for Sample 7 in the crystallization vicinity.

Comparison of these results with those previously obtained with bulk amorphous V_2O_5 indicates that the conductivity in our materials can be understood in the frame of the small-polaron theory. The semiconducting properties of amorphous V_2O_5 are due to a hopping process of unpaired electrons between V^{4+} and V^{5+} ions. They are usually described by the small-polaron model developed by Mott [24–28]:

$$\sigma = \frac{\nu_0 e^2}{RkT} C(1 - C) \exp(-2\alpha R) \exp(-W/kT)$$

where ν_0 is a phonon frequency, R the average hopping distance, C the ratio V^{4+}/V and α the rate of the wave-function decay. The activation energy W for the conductivity can be expressed as: $W = W_h + (1/2)W_d$, where W_h is the polaronic term while W_d corresponds to the random disorder.

It is usually very difficult to separate the terms W_h and W_d. It is commonly assumed that the polaronic term W_h is almost constant for all amorphous V_2O_5 thin films. The increase of the measured activation energy W should then be due mostly to an increase of the disorder term W_d. Electrical conductivity experiments then show that the disorder increases when the temperature of the substrate decreases, i.e. with an increasing fast quench rate of the vapour. A rough estimation of W_h and W_d was made for Sample 7, leading to $W_h = 0.18$ eV and $W_d = 0.17$ eV. Table II reports the values of $W = W_h + (1/2)W_d$ for Samples 1 to 5, in the 250–386 K temperature range. Particularly

TABLE II

Sample	W (eV)	Remark
1	0.54	
2	0.45	Increasing quenching
3	0.36	
4	0.32	
5	0.29	

significant is the increase of W, in agreement with the increasing rapid quenching of the vapour. Further calculations are being carried out in order to reach the exact values of both W_h and W_d for Layers 1 to 5.

4. Conclusion

The results described above show that vapour deposition gives a high efficiency of quenching, with the weakest quenching in this method corresponding to the highest one obtained by splat-cooling. As a consequence, non-equilibrium amorphous materials are obtained, which are characterized by the highest crystallization temperature even found for V_2O_5. This high temperature of crystallization in turn allows the detection of the glassy transition.

Acknowledgement

Several illuminating discussions with Dr R. Clement are gratefully acknowledged.

References

1. L. RIVOALEN, A. REVCOLEVSCHI, J. LIVAGE and R. COLLONGUES, *J. Non-Cryst. Sol.* **21** (1976) 171.
2. N. GHARBI, Thèse de 3e Cycle, Paris VI (1979).
3. J. BULLOT, O. GALLAIS, M. GAUTHIER and J. LIVAGE, *Appl. Phys. Lett.* **36** (1980) 986.
4. B. ARAKI, J. P. AUDIERE, M. MICHAUD and J. LIVAGE, *Bull. Soc. Chim.* **13** (1981) 9.
5. K. BALI, L. MICHAILOVITS and I. HEVESI, *Acta Phys. Chem.* **25** (1979) 44.
6. T. SZÖRENYI, K. BALI and I. HEVESI, *J. Non-Cryst. Sol.* **35–36** (1980) 1245.
7. G. A. ROZGONYI and W. J. POLITO, *J. Electrochem. Soc.* **115** (1968) 1245.
8. T. ALLERMA, R. HAKIM, T. N. KENNEDY and J. D. MACKENZIE, *J. Chem. Phys.* **46** (1967) 154.
9. F. P. KOFFYBERG and F. A. BENKO, *Phil. Mag. B* **38** (1978) 357.
10. T. N. KENNEDY, R. HAKIM and J. D. MACKENZIE, *Mater. Res. Bull.* **2** (1967) 193.
11. J. P. AUDIERE, C. MAZIERES and J. C. CARBALLES, *J. Non-Cryst. Sol.* **27** (1978) 411.
12. E. F. MILAN, *J. Phys. Chem.* **33** (1929) 498.
13. J. P. AUDIERE, Thèse de Doctorat d'Etat, Université Paris Sud (March 1978).
14. K. A. WILHELMI and K. WALTERSSON, *Acta Chem. Scand.* **24** (1970) 3409.
15. S. ANDERSSON, J. GALY and K. A. WILHELMI, *ibid* **24** (1970) 1473.
16. F. AEBI, *Helv. Chim. Acta* **31** (1948) 8.
17. N. GHARBI, C. R'KHA, D. BALLUTAUD, M. MICHAUD, J. LIVAGE, J. P. AUDIERE and G. SCHIFFMACHER, *J. Non-Cryst. Sol.* **46** (1981) 247.
18. J. P. AUDIERE, J. C. CARBALLES and C. MAZIERES, *J. Thermal Anal.* **6** (1974) 27.
19. C. MAZIERES, *Ann. Chem.* **36** (1964) 602.
20. J. P. AUDIERE, C. MAZIERES and J. C. CARBALLES, *J. Non-Cryst. Sol.* **34** (1979) 37.
21. National Bureau of Standards, Circular 8 (1958) 539.
22. R. C. WEAST (ed.), "Handbook of Chemistry and Physics" 51st edition (Chemical Rubber Co., 1970–1, Cleveland, Ohio) B.152.
23. C. SANCHEZ, private communication (1982).
24. N. F. MOTT, *J. Non-Cryst. Sol.* **1** (1968) 1.
25. A. P. SCHMID, *J. Appl. Phys.* **39** (1968) 3140.
26. T. HOLSTEIN, *Ann. Phys.* **8** (1959) 325.
27. *Idem, ibid* 8 (1959) 343.
28. N. F. MOTT and I. G. AUSTIN, *Adv. Phys.* **18** (1969) 41.

Received 8 March and accepted 19 March 1982